# Internalization is required for proper Wingless signaling in *Drosophila melanogaster*

Elaine S. Seto[3] and Hugo J. Bellen[1,2,3]

[1]Department of Molecular and Human Genetics and [2]Department of Neuroscience, Howard Hughes Medical Institute, and [3]Program in Developmental Biology, Baylor College of Medicine, Houston, TX 77030

The Wnt–Wingless (Wg) pathway regulates development through precisely controlled signaling. In this study, we show that intracellular trafficking regulates Wg signaling levels. In *Drosophila melanogaster* cells stimulated with Wg media, dynamin or Rab5 knockdown causes reduced Super8XTOPflash activity, suggesting that internalization and endosomal transport facilitate Wg signaling. In the wing, impaired dynamin function reduces Wg transcription. However, when Wg production is unaffected, extracellular Wg levels are increased. Despite this, target gene expression is reduced, indicating that internalization is also required for efficient Wg signaling in vivo. When endosomal transport is impaired, Wg signaling is similarly reduced. Conversely, the expression of Wg targets is enhanced by increased transport to endosomes or decreased hepatocyte growth factor–regulated tyrosine kinase substrate–mediated transport from endosomes. This increased signaling correlates with greater colocalized Wg, Arrow, and Dishevelled on endosomes. As these data indicate that endosomal transport promotes Wg signaling, our findings suggest that the regulation of endocytosis is a novel mechanism through which Wg signaling levels are determined.

## Introduction

During development, precisely regulated signaling pathways instruct cells to adopt particular fates. Wnt signaling mediates many developmental decisions (Wodarz and Nusse, 1998). Highlighting its importance, the misregulation of Wnt signaling causes improper fate specification, tumor formation, and early lethality (Cadigan and Nusse, 1997). Although proper Wnt signaling is essential, the mechanisms that control ligand distribution and signaling levels are not fully understood.

One process proposed to affect Wnt signaling is intracellular transport (Fig. 1 A; for review see Seto and Bellen, 2004). In endocytosis, membrane proteins are recruited to small plasma membrane invaginations. These forming endocytic vesicles are cleaved from membranes via the function of dynamin (Hinshaw, 2000), a protein encoded by *shibire* (*shi*) in *Drosophila melanogaster*. These vesicles then undergo Rab5-mediated fusion with the early endosome (Gorvel et al., 1991; Bucci et al., 1992). There, internalized proteins are sorted and redistributed within the cell. Proteins slated for degradation are sorted by hepatocyte growth factor–regulated tyrosine kinase substrate (Hrs) into the inner vesicles of the multivesicular body (MVB; Lloyd et al., 2002). When MVBs fuse with lysosomes, these internalized proteins are degraded.

Work in other signaling pathways has suggested that by regulating the level and distribution of ligand, endocytosis can affect the induction of signaling (Seto et al., 2002; for review see Seto and Bellen, 2004). Indeed, studies examining the relationship between endocytosis and Wingless (Wg) signaling suggest effects on Wg levels and spread. In the wing, loss of dynamin eliminates extracellular Wg (Wg(ex)) in 50% of samples (Strigini and Cohen, 2000), suggesting that dynamin may mediate Wg secretion. However, other studies indicate that dynamin is not involved in forming secretory vesicles from the Golgi (van der Bliek et al., 1993; Altschuler et al., 1998; Kasai et al., 1999). Thus, the effect of dynamin on Wg production remains unclear.

After Wg is secreted, it must travel to reach target cells. The role of endocytosis in Wg spread is heavily debated, as Wg may spread by either diffusion or intracellular transport. Supporting extracellular spread, dynamin-mediated internalization is not required for Wg spread in the wing (Strigini and Cohen, 2000). The efficiency of diffusion has been questioned, however, because Wg interacts with proteins in the extracellular matrix (Blair, 2005). Alternatively, Wg may spread through vesicle intermediates. GFP-tagged Wg can be internalized and recycled to

Correspondence to Hugo J. Bellen: hbellen@bcm.tmc.edu

Abbreviations used in this paper: Arm, Armadillo; Arr, Arrow; Ck1a, casein kinase 1a; CMV, cytomegalovirus; Dll, Distal-less; Dsh, Dishevelled; dsRNA, double-stranded RNA; DV, dorsal–ventral; Hrs, hepatocyte growth factor–regulated tyrosine kinase substrate; MVB, multivesicular body; RL, Renilla luciferase; Sens, Senseless; *shi*, *shibire*; Wg, Wingless; Wg(ex), extracellular Wg.

The online version of this article contains supplemental material.


The Journal of Cell Biology, Vol. 173, No. 1, April 10, 2006 95–106
http://www.jcb.org/cgi/doi/10.1083/jcb.200510123

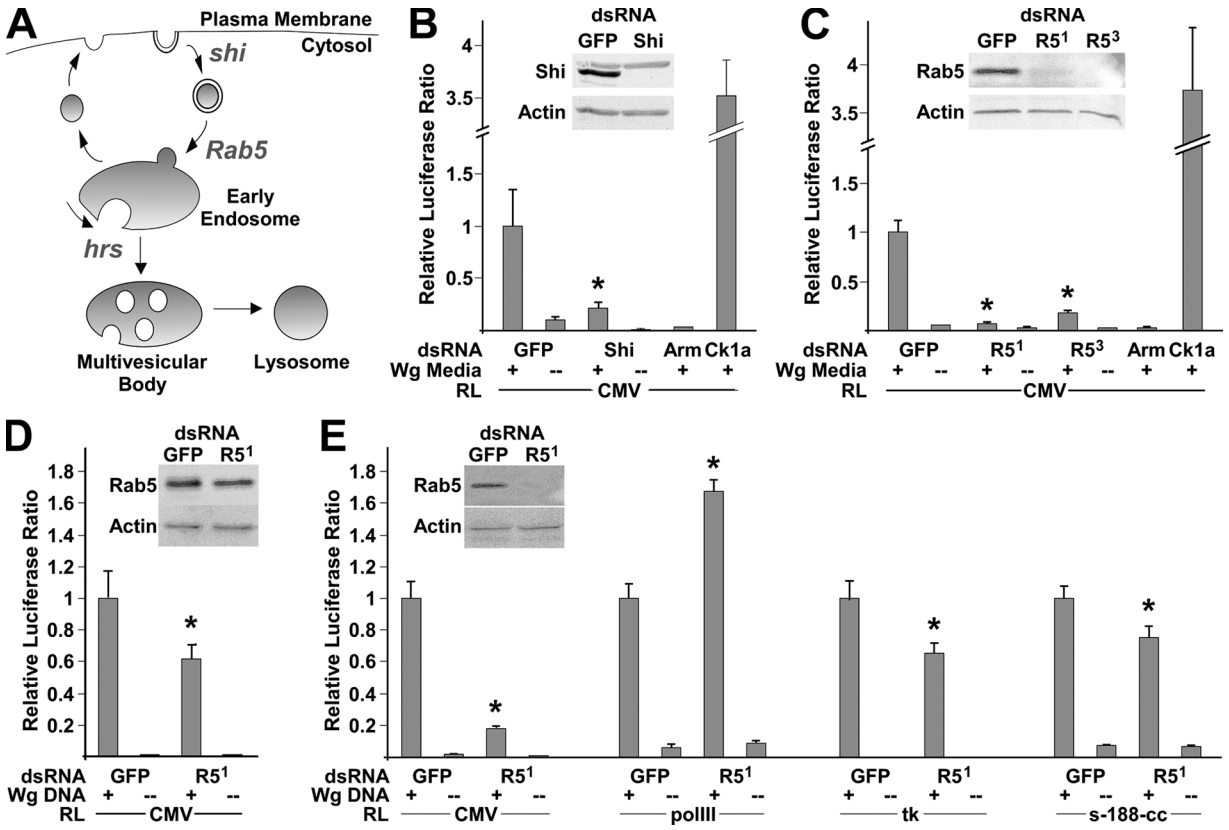


Figure 1. **Analysis of endocytic effects on Wg signaling in cell culture.** (A) Diagram of endocytosis. The function of *shibire* (*shi*), *Rab5*, and *hepatocyte growth factor–regulated tyrosine kinase substrate* (*hrs*) are altered in this work. (B) Relative Super8XTOPFlash/RL ratios 8 d after transfection with Super-8XTOPFlash, pCMV-RL, and dsRNA against EGFP, *shi*, *arm*, and *ck1a*. Wg media was added 1 d before cell lysis to induce signaling. Knockdown of dynamin (Shi) causes a significant reduction in luciferase ratio (*, $P < 0.05$). (C) Relative Super8XTOPFlash/RL ratios 8 d after transfection with Super8XTOPFlash, pCMV-RL, and dsRNA against EGFP, the Rab5 coding domain ($R5^1$), the Rab5 3′ untranslated region ($R5^3$), *arm*, and *ck1a*. Wg media was added 1 d before cell lysis to induce signaling. Knockdown of Rab5 by either $R5^1$ or $R5^3$ causes a significant reduction in luciferase ratio compared with controls (*, $P < 0.01$). (D) Relative Super8XTOPFlash/RL ratios 4 d after transfection with Super8XTOPFlash, pCMV-RL, pMK33-Wg, and dsRNA against EGFP and Rab5. The weak knockdown of Rab5 observed at this time point was sufficient to cause a statistically significant reduction in luciferase ratio (*, $P < 0.05$). (E) Relative Super8XTOPFlash/RL ratios 8 d after transfection with Super8XTOPFlash, pMK33-Wg, dsRNA against EGFP and Rab5, and various RL transfection control vectors. Transfection with pCMV-RL results in the strong knockdown of Rab5 and a dramatic reduction in luciferase ratio (*, $P < 0.01$). Transfection with polIII-RL, however, causes an increase in luciferase ratio that is consistent with other data (*, $P < 0.01$; DasGupta et al., 2005). Transfection with tk-RL and s-188-cc-RL both result in modest but statistically significant reductions in luciferase ratios (*, $P < 0.05$). Error bars represent SEM.

the cell surface in embryonic cells (Pfeiffer et al., 2002). Visualization of membrane phospholipids also suggests that Wg may spread via vesicular structures in the wing (Greco et al., 2001). Given that evidence supporting both extracellular and intracellular transport exists, the extent to which endocytosis affects Wg spread is controversial. Thus, although previous studies suggest that endocytosis may regulate Wg levels and spread (for review see Seto and Bellen, 2004), many questions remain.

Aside from affecting ligand levels and distribution, endocytosis may also regulate signal transduction (Di Fiore and De Camilli, 2001; Miaczynska et al., 2004). Determining whether endocytosis directly affects Wg signal transduction has been complicated, however, by difficulties in distinguishing effects on protein levels from signaling levels. In *shi* mutant embryos, Armadillo (Arm) staining is reduced but not eliminated (Bejsovec and Wieschaus, 1995). The presence of Arm indicates that Wg signaling can occur at the cell surface; however, it is unclear whether the reduction is caused by altered Wg spread or impaired signal transduction. Although this is consistent with the facilitation of Wg signaling by dynamin, it has been suggested that signaling is negatively regulated by Rab5 (DasGupta et al., 2005), raising doubt as to the necessity of endocytosis in Wg signaling. Given these contradictory results, the effect of endocytosis on Wg signaling is unclear.

In this study, we use genetic tools to alter vesicle transport and study the effect on Wg production, transport, degradation, and signaling. In *Drosophila* cells treated with Wg media, the knockdown of dynamin or Rab5 reduces Wg reporter activity, suggesting that internalization and endosomal transport facilitate signaling. In the wing, we find that dynamin mediates Wg transcription but is not required for Wg secretion or spread. Independent of altered Wg protein levels, endocytosis appears to regulate Wg signaling. Although impaired internalization and endosomal fusion increase Wg levels, signaling is reduced. Conversely, increased endosomal transport and obstructed transport from the endosome enhance Wg signaling. This correlates with the presence of endosomal accumulations of Wg, Arrow (Arr), and Dishevelled (Dsh). Thus, our data suggest that trafficking to the endosome facilitates Wg signaling possibly through the formation of an endosomal protein complex.

## Results

### Impaired endocytosis affects Wg signaling in cell culture

To determine endocytic effects on Wg signaling, a cell-based Wg assay was used. *Drosophila* S2R+ cells were transfected with a cytomegalovirus (CMV)-driven Renilla luciferase (RL) transfection control and Super8XTOPFlash (TOPFlash), a Wg reporter driving the expression of firefly luciferase. In response to Wg, the TOPFlash/RL ratio increases, serving as a quantitative measure of Wg signaling. Additionally, cells were transfected with double-stranded RNA (dsRNA) to determine the effect of particular genes on signaling. Knockdown of Arm, a mediator of Wg signaling, profoundly reduces TOPFlash/RL (Fig. 1, B and C; and Table S2, available at http://www.jcb.org/cgi/content/full/jcb.200510123/DC1). Conversely, knockdown of casein kinase 1a (ck1a), a negative regulator of signaling, strongly increases TOPFlash/RL (Fig. 1, B and C; and Table S2). These signaling levels are consistent with prior cell culture (Lum et al., 2003; DasGupta et al., 2005) and in vivo analyses (for review see van den Heuvel et al., 1993; Peifer et al., 1994).

We next transfected cells with dsRNA against the *shi* coding region. Wg media was added 7 d after transfection to induce signaling. Luciferase levels and protein knockdown were assessed on day 8. In stimulated cells with reduced dynamin, TOPFlash/RL decreased by 79% (Fig. 1 B and Table S2 A), indicating that dynamin promotes Wg signaling.

Similarly, the effects of endosomal transport were evaluated by transfection with dsRNA against the Rab5 coding region ($R5^1$; DasGupta et al., 2005). These cells showed a 93% decrease in luciferase ratio (Fig. 1 C and Table S2 B). This is surprising because a recent study argues that $R5^1$ transfection increases Wg signaling (DasGupta et al., 2005). To understand this discrepancy, we first reduced Rab5 using a dsRNA against the highly specific 3′ untranslated region ($R5^3$). Similar to $R5^1$, $R5^3$-treated cells show an 82% decrease in TOPFlash/RL (Fig. 1 C and Table S2 B). Second, we transfected cells with a Wg DNA construct, as performed by DasGupta et al. (2005), in lieu of adding Wg media. We initially examined cells 4 d after transfection as performed by DasGupta et al. (2005). Although Rab5 was still present at this time point (Fig. 1 D), a 38% reduction in TOPFlash/RL was observed (Fig. 1 D and Table S2 C). At 8 d after transfection, we observe strong knockdown and an 82% reduction in luciferase ratio, which is consistent with our results (Fig. 1 E and Table S2 D). Finally, we examined TOPFlash/RL ratios upon transfection with different RL control vectors (Fig. 1 E and Table S2 D). Although cells transfected with the polIII-RL transfection control used by DasGupta et al. (2005) show a 68% increase in luciferase ratio, transfection with tk-RL and s-188-cc-RL show 34 and 25% reductions in luciferase ratio, respectively. These varied TOPFlash/RL ratios indicate that transfection control vectors can produce different RL levels that dramatically impact the quantification of Wg signaling. However, given that $R5^1$ transfections with three out of four RL vectors show reduced luciferase ratios, our data suggest that impaired Rab5-mediated endosomal fusion hinders Wg signaling.

### Assessing Wg signaling activity in vivo

To determine the relevance of our cell culture data, we studied the effects of endocytosis on signaling in the wing. Wg forms a morphogen gradient in the larval wing that regulates proliferation and cell fate specification (Zecca et al., 1996; Neumann and Cohen, 1997). Wg is secreted at the dorsal–ventral (DV) boundary of the wing disc and is detected at high levels spanning approximately three cell widths (Baker, 1988; Couso et al., 1993; Williams et al., 1993). Spots of Wg are also present in the wing pouch, decreasing with distance from the DV boundary. As a morphogen, Wg can induce different target genes depending on signaling levels (Fig. 2 A). High levels of signaling induce Senseless (Sens) in cells bordering the DV boundary (Parker et al., 2002; Lin et al., 2003). Low levels of signaling are sufficient to induce Distal-less (Dll) broadly across the wing pouch (Diaz-Benjumea and Cohen, 1995; Zecca et al., 1996; Neumann and Cohen, 1997). Both Sens and Dll function in wing margin bristle development (Gorfinkiel et al., 1997; Nolo et al., 2000). Formation of a normal-sized wing is also dependent on Wg signaling, as *wg* mutants lack wings (Sharma and Chopra, 1976). Thus, by examining the expression of Wg targets and adult wing morphology, we can assess Wg signaling levels.

### Dynamin regulates Wg protein levels

To study the effect of internalization on signaling, we expressed dominant-negative *shi* ($shi^{DN}$) to impair internalization from the cell surface (Moline et al., 1999). Because it has been suggested that dynamin mediates Wg secretion (Strigini and Cohen, 2000), we used two Gal4 drivers to analyze Wg distribution and signaling. *C96-Gal4* induces expression at and near the DV boundary (Fig. 2 B; Gustafson and Boulianne, 1996), thereby permitting analysis of Wg transcription and secretion. Conversely, *C5-Gal4* (Yeh et al., 1995) induces expression throughout the wing pouch except for cells at the DV boundary (Fig. 2 C). Because this does not include Wg-expressing cells, *C5-Gal4* allows analysis of Wg spread and degradation independent of Wg production. By combining data from these drivers, we can study changes in Wg production, spread, degradation, and signaling.

When $shi^{DN}$ was overexpressed at the DV boundary, Wg distribution is narrow compared with controls (Fig. 2, D and E), which is indicative of altered Wg transcription or secretion. In situs show less Wg RNA (Fig. 2 I), indicating that dynamin facilitates Wg transcription likely through its regulation of Notch signaling (Diaz-Benjumea and Cohen, 1995; Rulifson and Blair, 1995; Seugnet et al., 1997). However, as shown in Fig. 2 M, *C96-Gal4/UAS-*$shi^{DN}$ discs exhibit elevated Wg(ex) levels compared with controls. Thus, our data suggest that when dynamin function is blocked, Wg transcription is reduced, but Wg is secreted and accumulates extracellularly.

To investigate the effect of dynamin on Wg spread, we expressed $shi^{DN}$ using *C5-Gal4*. These discs show a dramatically widened Wg distribution compared with controls (Fig. 2, F and G). Consistent with impaired internalization, this protein can be detected extracellularly (Fig. 2 O). Because Wg expression is similar to controls (Fig. 2 K), the enhanced Wg(ex) likely results from reduced Wg degradation when *shi* function is inhibited. Notably, the normal Wg expression also indicates that Wg can

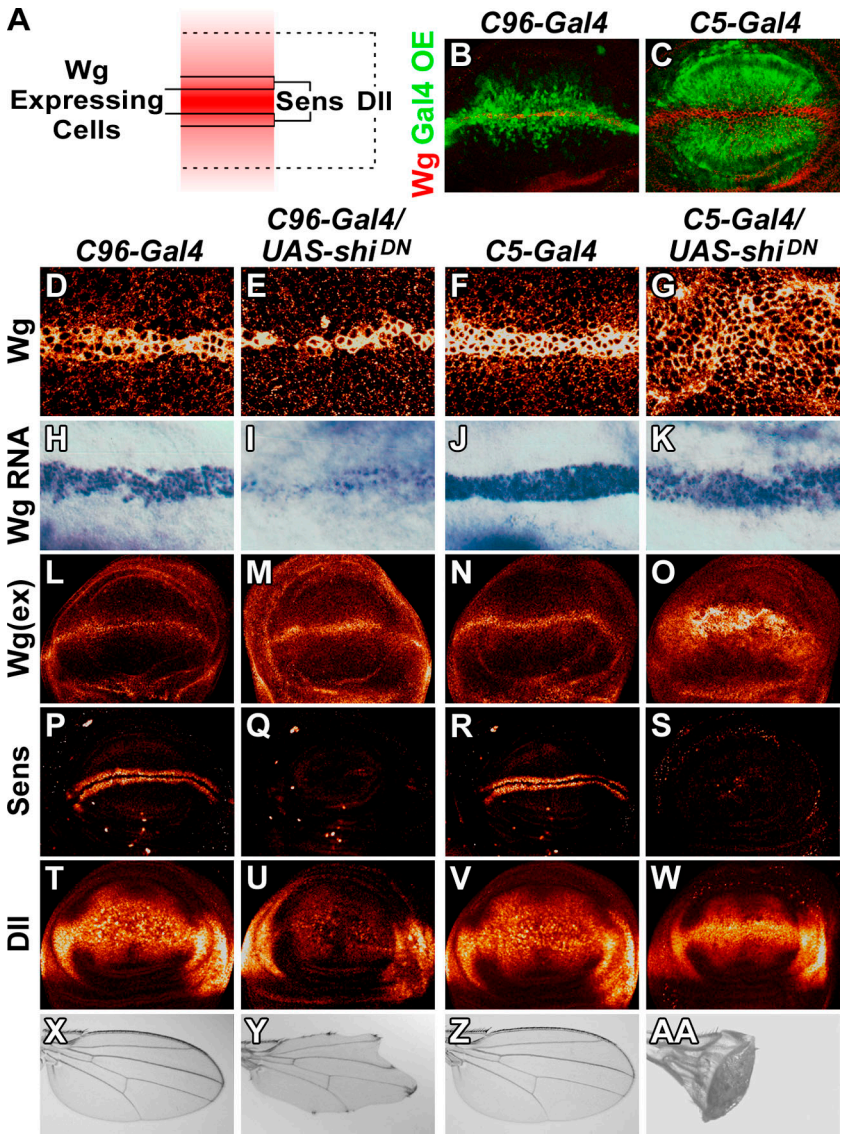


Figure 2. **Effects of impaired dynamin function on Wg signaling in vivo.** (A) Diagram of the Wg morphogen gradient. Wg is secreted from cells at the DV boundary and spreads across the wing disc. Depending on the level of signaling, different target genes are expressed. High levels of Wg induce the expression of Sens around the DV boundary. Moderate levels of Wg are sufficient to induce Dll in a broad domain across the wing pouch. (B and C) Expression patterns of *C96-Gal4* and *C5-Gal4* in the third instar wing discs shown by β-galactosidase staining (green). The DV boundary is labeled for reference by high Wg levels (red). C96-Gal4 is expressed in cells at and near the DV boundary, whereas *C5-Gal4* is expressed throughout the wing pouch, with the exception of cells at the DV boundary. (D–AA) Analysis of Wg distribution and signaling when dominant-negative *shi* ($shi^{DN}$) is expressed. (D–G) Conventional Wg staining. When dynamin function is impaired near the DV boundary, the width of Wg distribution is reduced. When dynamin function is impaired in the wing pouch, the width of Wg protein distribution is dramatically expanded (G). (H–K) Wg in situ hybridization. Impaired dynamin function reduces endogenous Wg transcription. (L–O) Wg(ex) staining. Inhibition of dynamin function results in increased Wg(ex) levels, suggesting that Wg secretion is not blocked. This further indicates that internalization down-regulates ligand levels. Despite the increased levels of Wg(ex), the expression of Sens (P–S) and Dll (T–W) appear reduced. (X–AA) The adult wings exhibit a loss of wing tissue and bristles, which is consistent with decreased Wg signaling.

spread from the DV boundary in a dynamin-independent manner. Thus, dynamin regulates Wg levels through transcription and degradation but does not appear to be required for Wg secretion or spread.

### Wg signaling is negatively regulated by dynamin

To determine whether dynamin affects signaling, Wg target gene expression was examined. Although both *C96-Gal4* and *C5-Gal4* overexpression of $shi^{DN}$ show enhanced levels of Wg(ex), we find that Sens expression is nearly absent (Fig. 2, P–S), indicating that dynamin is required to achieve high signaling levels. Furthermore, Dll levels in $shi^{DN}$ cells are decreased compared with cells outside the wing pouch that do not express $shi^{DN}$ (Fig. 2, T–W). Dll expression is similarly reduced in temperature-sensitive *shi* ($shi^{ts1}$) mutant clones at the restrictive temperature (not depicted). The progressively weaker effects of dynamin on Sens and Dll are consistent with our understanding of the Wg morphogen gradient and indicate that impaired internalization reduces but does not eliminate Wg signaling. Notably, the reduced protein expression is unlikely to be the result of cell death, as little to no TUNEL-positive columnar cells are observed in the *C96-Gal4/UAS-*$shi^{DN}$, *C5-Gal4/UAS-*$shi^{DN}$, and $shi^{ts1}$ discs studied (Fig. S1, B and C; available at http://www.jcb.org/cgi/content/full/jcb.200510123/DC1). Additionally, the differential decrease in Sens and Dll suggests that these reductions do not arise from cell death. Further supporting reduced Wg signaling, *C96-Gal4/UAS-*$shi^{DN}$ wings show a loss of margin tissue that resembles the *wg* mutant phenotype (Fig. 2 Y; Baker, 1988; Couso et al., 1994; Diaz-Benjumea and Cohen, 1995). *C5-Gal4/UAS-*$shi^{DN}$ adult wings are small with altered morphology (Fig. 2 AA), exhibiting bristle loss consistent with decreased Sens expression and Wg signaling (Phillips and Whittle, 1993; Couso et al., 1994). Thus, consistent with our cell culture data, these data indicate that impaired dynamin function reduces Wg signaling even when significantly more Wg(ex) is present. This effect is more obvious for Wg targets requiring high signaling levels, suggesting that Wg(ex) can induce only low signaling levels in the absence of dynamin-mediated internalization.

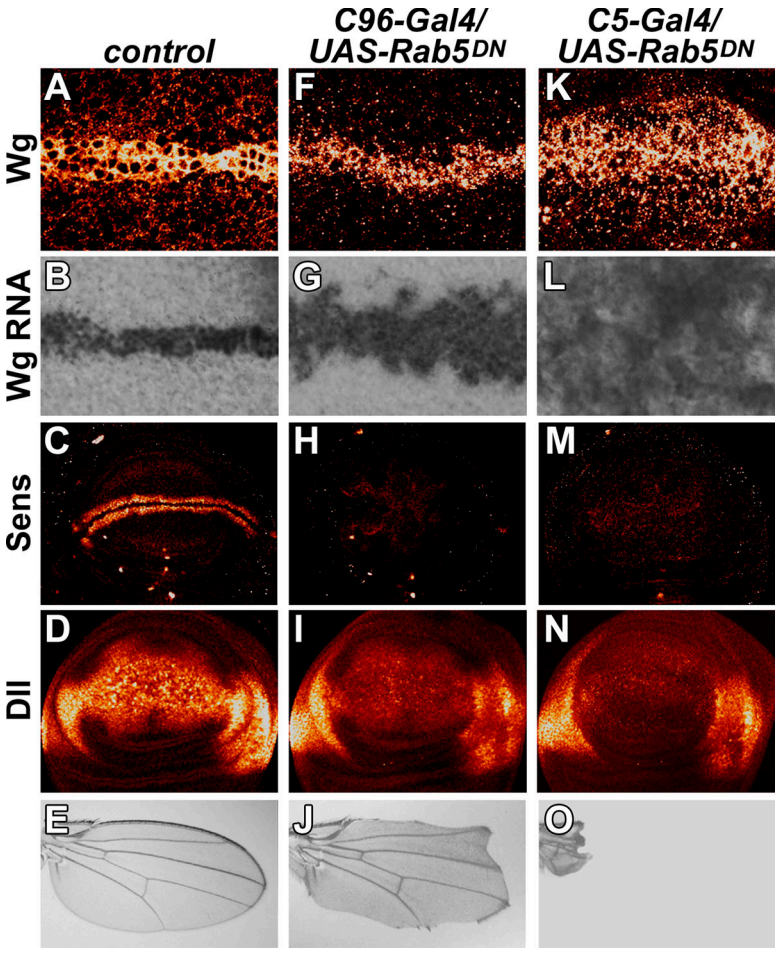


Figure 3. **Inhibition of early endosomal fusion reduces Wg signaling.** (A–E) As *C96-Gal4* and *C5-Gal4* produce no phenotypes, representative control images are shown. (F–J) *UAS-Rab5$^{SN}$/+; C96-Gal4/+* overexpression of dominant-negative *Rab5* inhibits endosomal fusion around the DV boundary. Wg distribution and transcription are normal or slightly enhanced (F and G); however, the expression of Wg signaling targets is reduced (H and I). The adult wing shows a loss of wing margin tissue that is consistent with decreased Wg signaling (J). (K–O) *UAS-Rab5$^{SN}$/+; C5-Gal4/+* overexpression of dominant-negative *Rab5* in the wing pouch. Wg protein levels and transcription are increased (K and L). However, the expression of Sens (M) and Dll (N) are reduced. The adult wing is almost completely absent (O), which is similar to *wg* mutants.

### Endosomal trafficking promotes Wg signaling

After dynamin-mediated internalization, endocytic vesicles undergo Rab5-mediated fusion with the endosome (Gorvel et al., 1991; Bucci et al., 1992). As our cell culture data suggest that the loss of Rab5 reduces Wg signaling, we determined whether endosomal transport affects signaling in vivo by expressing dominant-negative Rab5 (Rab5$^{DN}$, also called Rab5$^{SN}$), a constitutively GDP-bound form that inhibits endosomal fusion (Stenmark et al., 1994; Entchev et al., 2000). In *C96-Gal4/UAS-Rab5$^{DN}$* discs, Wg staining is more punctate but otherwise similar to controls (Fig. 3 F). Despite this, Sens expression near the DV boundary is eliminated (Fig. 3 H), indicating that high levels of signaling are blocked by impaired endosomal transport. Dll expression is also much reduced compared with levels outside of the wing pouch (Fig. 3 I). The stronger effect on Sens than Dll is similar to *shi$^{DN}$*, further indicating that high Wg signaling levels cannot be reached when endocytosis is blocked. Evaluating cell death, we find TUNEL-positive columnar cells upon the *C96-Gal4* expression of *Rab5$^{DN}$* (Fig. S1 D). However, this cell death likely causes only minor changes in protein expression as indicated by the large number of Wg-expressing cells present (Fig. 3 G). Additionally, *C96-Gal4* overexpression of *Rab5$^{DN}$* results in the loss of wing tissue similar to the loss of Wg (Baker, 1988; Couso et al., 1994; Diaz-Benjumea and Cohen, 1995), further suggesting that endosomal transport significantly affects Wg signaling. Similarly, we have analyzed the *C5-Gal4* expression of *Rab5$^{DN}$*. As shown in Fig. 3 K, Wg distribution is significantly expanded, which was caused, in part, by increased Wg transcription (Fig. 3 L). Despite high Wg levels, Sens expression is absent, and Dll expression is markedly reduced (Fig. 3, M and N). Again, the differential effects on Sens and Dll expression are consistent with impairment of the Wg signaling gradient. *C5-Gal4* expression of *Rab5$^{DN}$* causes almost a complete loss of wing tissue (Fig. 3 O), as documented for *wg* mutants (Sharma and Chopra, 1976). Notably, coexpression of Arm (Pai et al., 1997), a mediator of Wg signaling, partially restores bristles and wing size (unpublished data). This indicates that although some TUNEL-positive cells are observed in columnar cells expressing Rab5$^{DN}$ (Fig. S1 D), cell death does not account for the observed phenotypes. Together, these data suggest that early endosomal transport facilitates Wg signaling in vivo.

Although Rab5$^{DN}$ is constitutively inactive, wild-type Rab5 (Rab5$^{WT}$) is subject to the regulation of cellular factors (Somsel Rodman and Wandinger-Ness, 2000). To examine the effect of Rab5$^{WT}$, we induced clones of the *Actin-Gal4* expression of *Rab5$^{WT}$*. As shown in Fig. 4 (A–C), Rab5$^{WT}$ overexpression causes no change in Wg, Sens, or Dll expression. Interestingly, it has been reported that *C96-Gal4* expression of Rab5$^{WT}$ decreases Sens levels (DasGupta et al., 2005). However, we find that the overexpression of Rab5$^{WT}$ by either *C96-Gal4* or

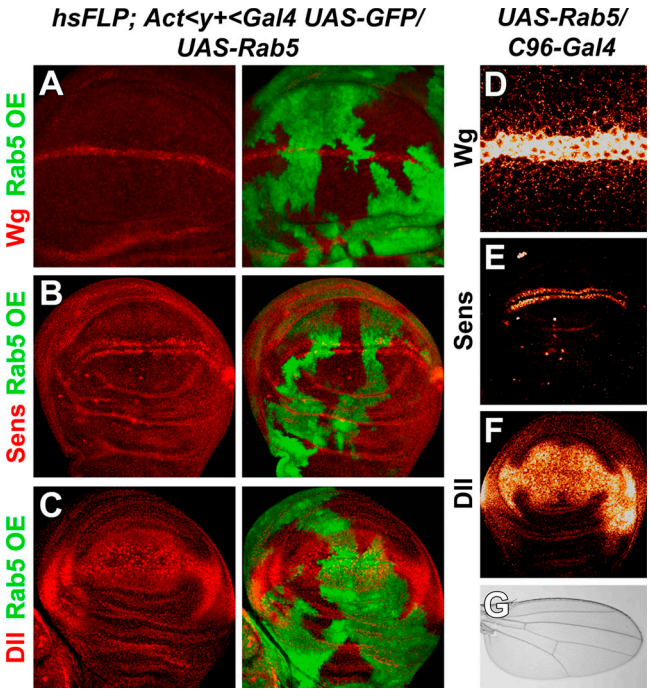


Figure 4. **Overexpression of wild-type Rab5 does not affect Wg signaling.** (A–C) Positively marked Rab5 overexpression (OE) clones. Staining for Wg (A), Sens (B), and Dll (C) reveals no difference in expression between wild-type and Rab5-overexpressing cells (green). (D–G) *C96-Gal5* overexpression of $Rab5^{WT}$ near the DV boundary. No difference in Wg (D), Sens (E), or Dll (F) expression is observed. Consistent with normal Wg signaling, the adult wing is indistinguishable from controls (G).

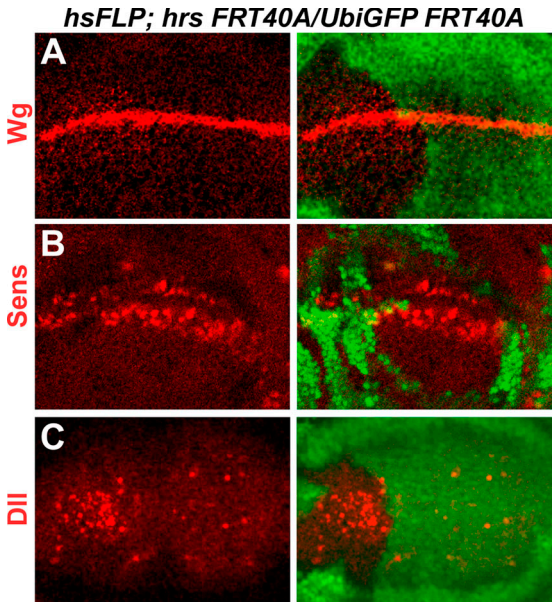


Figure 5. **Impaired trafficking from the endosome to the MVB enhances Wg signaling.** Projection view of $hrs^{D28}$ mutant clones marked by the absence of GFP expression (green). (A) Homozygous *hrs* mutant tissue exhibits a slightly expanded Wg distribution with large protein accumulations in the wing pouch. These puncta are not detected by extracellular staining (not depicted), indicating that they are intracellular. (B) Within *hrs* mutant clones, Sens expression is sometimes broadened. This is particularly evident within large clones. (C) The expression of Dll can also be enhanced within *hrs* mutant tissue. This is particularly evident within large clones.

*C5-Gal4* causes no change in Wg, Sens, or Dll expression (Fig. 4, D–F; and not depicted). Furthermore, the adult wings are indistinguishable from controls (Fig. 4 G and not depicted). These data indicate that $Rab5^{WT}$ overexpression does not change Wg signaling. Given the different results obtained from $Rab5^{DN}$ and $Rab5^{WT}$, our data also suggest that endocytic regulators can control Wg signaling by altering endosomal transport. Consistent with this, the overexpression of dominant active Rab5 ($Rab5^{DA}$, also called $Rab5^{QL}$) causes an enhancement in signaling that was not observed with either $Rab5^{DN}$ or $Rab5^{WT}$. In these discs, Sens expression is detected more than two cell diameters from the DV boundary, and Dll expression is enhanced in the Gal4 expression domain (Fig. S2, D–I; available at http://www.jcb.org/cgi/content/full/jcb.200510123/DC1). Consistent with increased Sens expression and Wg signaling (Brennan et al., 1999; Nolo et al., 2000), the adult wings develop ectopic bristles (Fig. S2, K and L). These data suggest that although $Rab5^{DN}$ expression reduces Wg signaling, the promotion of endosomal transport by $Rab5^{DA}$ enhances signaling. These data further indicate that in addition to proteins like dynamin and Rab5 that directly mediate vesicle trafficking, regulators of endocytic proteins can modulate Wg signaling.

## Trafficking to the MVB reduces Wg signaling

Upon internalization to the endosome, proteins slated for degradation are sorted into MVBs via the function of Hrs (Lloyd et al., 2002; Raiborg et al., 2002). We analyzed wings with altered Hrs function to determine whether trafficking from endosomes to MVBs affects signaling. In *hrs* mutant clones, Wg distribution is slightly expanded, with much of the protein localized in large puncta (Fig. 5 A; see Fig. 8 C). Wg(ex) staining fails to detect these accumulations (not depicted). Although most Wg is located intracellularly in *hrs* mutants, Sens is sometimes more broadly expressed within *hrs* mutant clones than in the internal control (Fig. 5 B). Similarly, some *hrs* mutant clones show enhanced Dll levels (Fig. 5 C). These changes in expression are most evident in large clones induced early in development. As Hrs is a very stable protein (Lloyd et al., 2002), small clones induced later show minor or no changes in Wg target gene expression, probably as a result of Hrs protein perdurance. Thus, although less Wg(ex) is present than in controls, the impairment of endosome to MVB transport augments Wg signaling.

Our data strongly suggest that internalization and protein localization to the early endosome play a critical role in Wg signaling. We next examined the effect of enhanced MVB transport. The overexpression of Hrs by *C96-Gal4* and *C5-Gal4* facilitates trafficking through MVBs as demonstrated by enlarged LAMP-positive lysosomes (not depicted). When Hrs is overexpressed at the DV boundary, Wg distribution is disrupted (Fig. 6 B). However, when Hrs is broadly expressed, Wg distribution is slightly widened (Fig. 6 C). Despite differences in Wg levels, both genotypes show a reduction in Sens and Dll (Fig. 6, D–I). Consistent with reduced signaling, *C96-Gal4 UAS-hrs* wings have a loss of margin tissue (Fig. 6 K), and *C5-Gal4 UAS-hrs* wings are reduced in size with fewer bristles near the wing margin (not depicted). Further supporting an effect on Wg signaling, the cooverexpression of Wg with Hrs largely suppresses the loss of

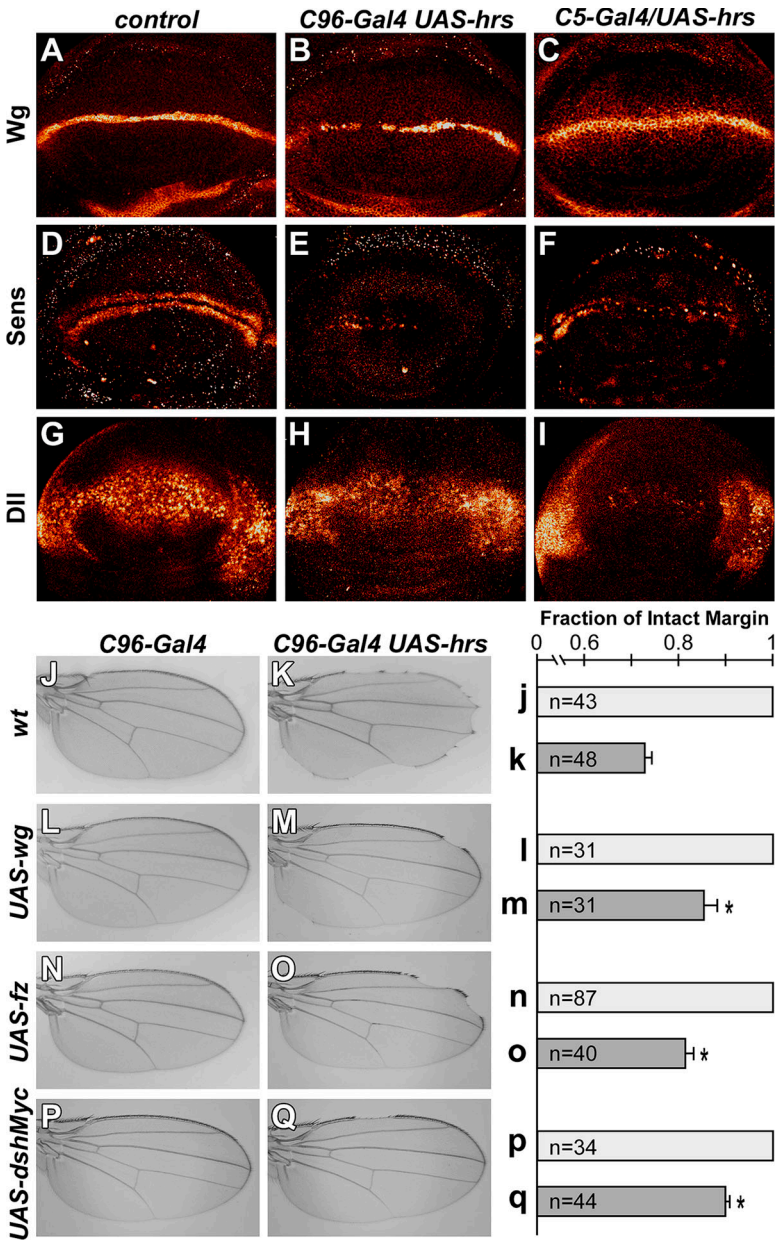


Figure 6. **Increased transport to the MVB negatively regulates Wg signaling.** (A–I) Analysis of Wg protein distribution and signaling upon Hrs overexpression. As *C96-Gal4* and *C5-Gal4* cause no phenotype, representative control images are shown. (A–C) Conventional Wg staining of *C96-Gal4 UAS-hrs* and *C5-Gal4/UAS-hrs* discs reveal reduced and normal Wg levels, respectively. (D–F) Sens expression is significantly reduced where Hrs is overexpressed. (G–I) Expression of Dll is also reduced. (J–Q) The adult wing phenotype of Hrs overexpression at the wing margin is specifically suppressed by the overexpression of Wg signaling components. (J) *C96-Gal4*. Wing shows an intact margin. (K) *C96-Gal4 UAS-hrs/TM6*. Overexpression of Hrs exhibits wing notching at 25°C, reducing the fraction of intact wing margin to 0.73 ± 0.02. (L) *C96-Gal4/UAS-wg*. Overexpression of Wg at 21°C shows an intact margin. (M) *C96-Gal4 UAS-hrs/UAS-wg*. Cooverexpression of Hrs and Wg at 21°C suppresses the wing notching observed from Hrs overexpression alone, increasing the fraction of intact wing margin to 0.85 ± 0.03. (N) *C96-Gal4/UAS-fz*. Overexpression of Frizzled at 25°C shows an intact margin. (O) *C96-Gal4 UAS-hrs/UAS-fz*. Cooverexpression of Hrs and Frizzled at 25°C suppresses the wing notching observed from Hrs overexpression alone, increasing the fraction of intact wing margin to 0.82 ± 0.02. (P) *Sp/+; C96-Gal4/UAS-dshMyc*. Overexpression of myc-tagged Dsh at 25°C shows an intact margin. (Q) *C96-Gal4 UAS-hrs/UAS-dshMyc*. Cooverexpression of Hrs and myc-tagged Dsh at 25°C suppresses the wing notching observed from Hrs overexpression alone, increasing the fraction of intact wing margin to 0.90 ± 0.01. Asterisks denote the significant suppression of the *C96-Gal4 UAS-hrs/TM6* phenotype ($P < 0.01$). Error bars represent SEM.

margin tissue (Fig. 6 M). In canonical Wg signaling, Wg associates with Frizzled receptors and Arr coreceptors to phosphorylate the cytoplasmic protein Dsh and activate signaling (Wodarz and Nusse, 1998; Tamai et al., 2000; Wehrli et al., 2000). We find that the coexpression of Frizzled (Fig. 6 O) and myc-tagged Dsh (Fig. 6 Q) are each capable of suppressing the *C96-Gal4 UAS-hrs* phenotype. These data indicate that Hrs phenotypes arise specifically from changes in Wg signaling rather than other factors (Fig. S1 G). Together, these data suggest that although internalization and early endosomal transport facilitate Wg signaling, progression to the MVB negatively regulates signaling.

### Wg signaling members are localized at early endosomes

Our data indicate that localization to early endosomes enhances Wg signaling. This is similar to receptor tyrosine kinase signaling, where the formation of endosomal signaling complexes is proposed to facilitate signaling (Lloyd et al., 2002; Miaczynska et al., 2004). To determine whether Wg signaling occurs in a similar manner, we first studied Wg localization. We find that Wg partially colocalizes with the early and late endosome marker FYVE-GFP (not depicted; Wucherpfennig et al., 2003) and the late endosomal protein Rab7-GFP (Fig. 7 A; Bucci et al., 2000). Additionally, electron microscopy was performed on wing discs expressing HRP-tagged Wg protein (Dubois et al., 2001). Based on compartment morphology, HRP activity is localized to small vesicles, endosomes, MVBs, and lysosomes (Fig. 7, B–E). Thus, Wg is internalized and trafficked through intracellular compartments.

We further examined the localization of Arr, the *Drosophila* homologue of LRP5/6, and Dsh, which are two proteins that are necessary for Wg signaling (Klingensmith et al., 1994; Theisen et al., 1994; Wehrli et al., 2000). In controls, small puncta of HA-tagged Arr (ArrHA) sometimes colocalize with

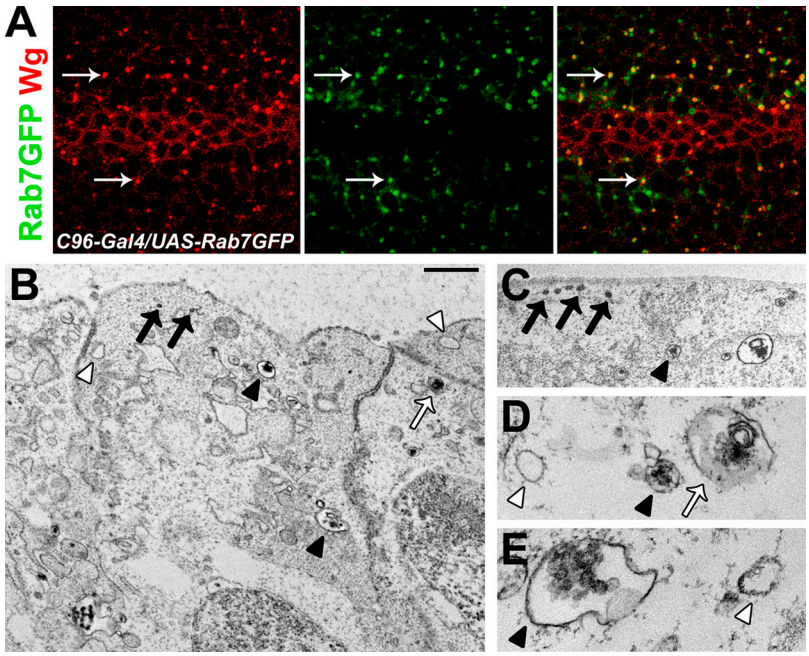


Figure 7. **Analysis of Wg intracellular transport.** (A) *C96-Gal4/UAS-Rab7GFP* wing discs stained for Wg protein (red). Arrows point to Wg colocalization with the late endosome marker GFP-tagged Rab7 (green). (B–E) Electron micrographs of third instar *C5-Gal4/UAS-wgHRP* wing discs stained with DAB. Black arrows point to HRP-positive small vesicles, white arrowheads point to endosomes, black arrowheads indicate MVBs, and white arrows point to lysosomes. These HRP-positive structures are not observed in control discs (not depicted). Bars (B and C), 1 μm; (D) 500 nm; (E) 200 nm.

Wg (Fig. 8 A). ArrHA and Wg also occasionally colocalize with Dsh, which is present at low levels in the cytoplasm as well as in small puncta (Fig. 8 B and not depicted). In *hrs* mutants, ArrHA and Wg often localize to large puncta that colocalize with the endosome/lysosome marker Benchwarmer (also called Spinster; Fig. 8, C and E; Sweeney and Davis, 2002; Dermaut et al., 2005). Intracellular ArrHA and Wg often also colocalize with accumulations of Dsh (Fig. 8, D and F; and not depicted). Thus, in *hrs* mutants, enhanced Wg signaling correlates with greater colocalized Wg, Arr, and Dsh on endosomes than in wild-type cells.

## Discussion

Our analysis has revealed the surprising finding that intracellular transport affects the efficiency of Wg signaling. In cell culture, knockdown of dynamin, a protein essential for clathrin-mediated internalization, reduces the TOPFlash/RL ratio, which is suggestive of decreased Wg signaling. Similarly, Rab5 knockdown causes reduced TOPFlash/RL ratios under most conditions, suggesting that internalization and endosomal transport are important for Wg signaling. Interestingly, transfection with polIII-RL, a control vector used in a recent screen for modifiers of Wg signaling (DasGupta et al., 2005), produces conflicting results for Rab5 compared with other RL controls, indicating that cell culture–based Wg signaling assays are very sensitive to experimental conditions. Thus, although our cell culture results indicate an endocytic regulation of Wg signaling, in vivo validation is critically important.

In the wing, we found further evidence that Wg signaling levels are highly dependent on intracellular transport. When endocytosis is altered, ligand levels and signaling levels are uncoupled such that high Wg levels do not necessarily enhance signaling. Therefore, we have limited usage of the term morphogen gradient, which could refer to either ligand or signaling levels. We instead describe Wg distribution and signaling readouts. When internalization is inhibited in a domain that does not affect Wg production, we find high levels of Wg(ex), likely as a result of reduced degradation. However, Wg target gene expression is diminished, indicating that impaired internalization decreases Wg signaling in vivo as well as in cell culture. When early endosomal transport is impaired, Sens and Dll expression are also reduced despite abundant Wg levels. In both cases, markers of high signaling levels are especially affected, indicating that intracellular signaling is important to achieve robust Wg signaling levels. The differential decrease also argues that changes in Sens and Dll expression are not merely the result of cell death or global changes in transcription (Piddini et al., 2005). Further supporting this, we find the normal expression of other genes in the wing pouch (unpublished data). Additionally, when endosomal transport is enhanced or when transport from the endosome is impaired, Wg signaling is increased. These data suggest that protein localization to the endosome facilitates Wg signaling. Conversely, increased transport to MVBs decreases the expression of Wg readouts. This causes an adult wing phenotype that can be suppressed by Wg signaling components. Thus, we propose that in addition to low levels of cell surface signaling, intracellular Wg signaling is critical for proper signaling levels (Fig. 9).

Because endocytosis is tightly regulated, intracellular Wg signaling may allow for the rapid modulation of signaling levels. For example, endosomal transport can be regulated merely by changing the GDP/GTP state of Rab5. Our work indicates that impaired endosomal transport by GDP-bound Rab5 reduces Wg signaling, whereas enhanced endosomal fusion by GTP-bound Rab5 increases signaling. Because the GDP/GTP-binding state of Rab5 is controlled posttranslationally by GTPase-activating proteins and guanine nucleotide exchange factors, endocytic regulation likely allows more of a rapid adjustment of signaling than regulatory mechanisms requiring transcription and translation. Furthermore, because endocytic rates vary between

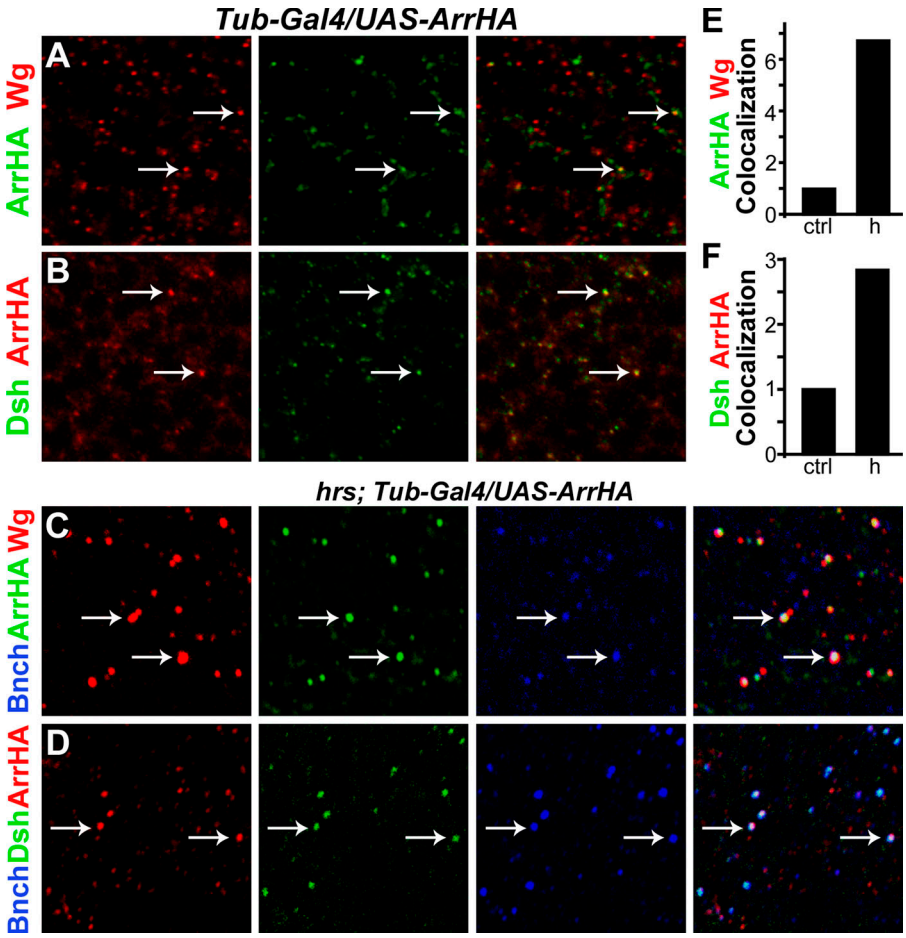


Figure 8. **Intracellular localization of Wg signaling components.** (A) *Tub-Gal4/UAS-ArrHA* wing discs stained for Wg (red) and the HA tag (green). Arrows point to puncta of Wg colocalization with HA-tagged Arr protein. (B) *Tub-Gal4/UAS-ArrHA* wing discs stained for the HA tag (red) and Dsh (green). Arrows point to colocalized HA-tagged Arr protein and Dsh. (C) $hrs^{D28}$*; Tub-Gal4/UAS-ArrHA* wing discs stained for Wg (red), the HA tag (green), and the endosomal marker Benchwarmer (blue). Arrows point to large puncta of Wg colocalization with HA-tagged Arr protein on endosomes. (D) $hrs^{D28}$*; Tub-Gal4/UAS-ArrHA* wing discs stained for the HA tag (red), Dsh (green), and the endosomal marker Benchwarmer (blue). Arrows point to large puncta of colocalized HA-tagged Arr protein and Dsh on endosomes. (E) Quantification of Wg and HA-tagged Arr colocalization in control and *hrs* mutant backgrounds. The $hrs^{D28}$*; Tub-Gal4/UAS-ArrHA* disc (C) shows 6.7 times the amount of colocalized pixels observed in the *Tub-Gal4/UAS-ArrHA* control (A). (F) Quantification of HA-tagged Arr and Dsh colocalization in control and *hrs* mutant backgrounds. The $hrs^{D28}$*; Tub-Gal4/UAS-ArrHA* disc (D) shows 2.8 times the number of colocalized pixels present in the *Tub-Gal4/UAS-ArrHA* control (B).

cell types, this regulation may allow signaling to be adjusted in particular parts of the body or cells of a tissue. Thus, regulated endocytosis allows for precise temporal and spatial control of Wg signaling.

Endocytosis is hypothesized to regulate signaling through several mechanisms. For example, lysosomal degradation of internalized active receptor tyrosine kinases serves to attenuate signaling (Lloyd et al., 2002; Seto et al., 2002). However, our data suggest that Wg signaling is enhanced by endocytosis. One theory by which intracellular transport facilitates signaling is that the internalization of ligand–receptor complexes promotes interactions with other signaling members recruited to or already present on endosomes. In MAPK signaling, ERK1 receptors form protein complexes with endosomal MP1 and p14 (Teis et al., 2002), leading to greater activation of signaling. Similarly, TGFβ signaling may be enhanced by receptor internalization to endosomes where the Smad2 anchor protein SARA is enriched (Seto et al., 2002). Although our work and that of others suggests that Wg undergoes receptor-mediated internalization in the wing (Piddini et al., 2005; Marois et al., 2006), these data alone cannot explain the enhanced Wg signaling observed. However, not only are Wg and Arr colocalized in large endosomal accumulations in *hrs* mutants, but they also colocalize with the cytoplasmic signaling component Dsh. The colocalization of Wg, Arr, and Dsh correlates with the increased expression of Wg readouts. These data suggest that internalization and

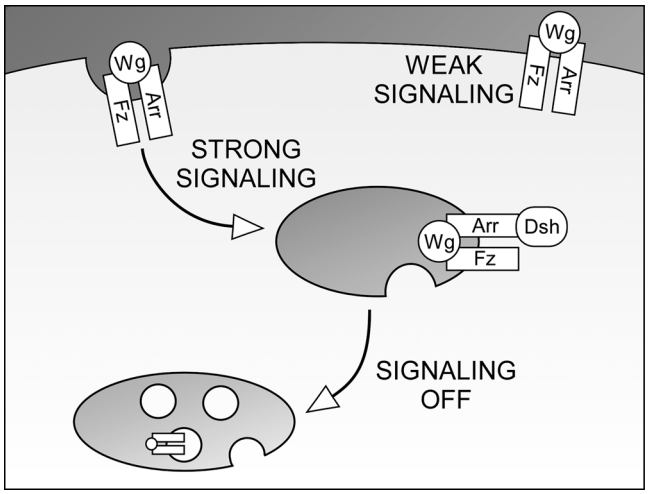


Figure 9. **Model of intracellular Wg signaling.** Based on the data obtained from altering endocytosis, Wg at the cell surface produces only low levels of Wg signaling in the wing. Wg associates with its receptors and is internalized. When endocytic vesicles fuse with the early endosome, the cytoplasmic domains of the Wg receptors Frizzled and Arr are able to associate with downstream signaling components like Dsh, thereby facilitating Wg signaling. Subsequent endosomal sorting into MVB inner vesicles sequesters the Wg–receptor complex from other signaling components, and the activation of signaling transduction is halted.

endosomal transport may promote Wg signaling by facilitating associations between the Wg–receptor complex and downstream signaling components like Dsh. Interestingly, Dsh is reportedly present on intracellular vesicles, and mutations that impair vesicular localization do disrupt canonical Wg signaling (for review see Seto and Bellen, 2004).

Axin, a protein that inhibits Wg signaling by downregulating Arm levels (Hamada et al., 1999), has also been shown to colocalize with Dsh on intracellular vesicles (Fagotto et al., 1999). Upon Wg signaling, Axin relocalizes from intracellular puncta to the plasma membrane (Cliffe et al., 2003). This correlates with Arm stabilization and increased Wg signaling. Because Axin associates with Dsh and the cytoplasmic tail of Arr (for review see Seto and Bellen, 2004), we propose that internalized Wg forms an endosomal signaling complex that may relocalize Axin, thereby stabilizing Arm and facilitating signaling.

## Materials and methods

### Cell culture transfections

*Drosophila* S2R+ cells express all of the signaling components necessary to respond to exogenously added Wg (Yanagawa et al., 1998), making them well suited to study Wg signaling. S2R+ cells (a gift from P. Beachy, Johns Hopkins University School of Medicine, Baltimore, MD) were maintained in Schneider's Media (Invitrogen) with 10% heat-inactivated FBS (JRH Biosciences). For protein knockdown, dsRNAs were synthesized using the MEGAscript RNAi kit (Ambion) from PCR products containing the T7 promoter (taatacgactcactataggg). Primer pairs are shown in Table S1 (available at http://www.jcb.org/cgi/content/full/jcb.200510123/DC1). Several transfection protocols were tested in this study. Amounts for six-well plate transfections are shown as follows: (1) 0.2 μg dsRNA, 0.2 μg Super8XTOPFlash or Super8XFOPFlash (Veeman et al., 2003), and 2 ng pRL-CMV (Promega) in 100 μL were sequentially combined with 3.2 μL Effectene Enhancer (QIAGEN), 10 μL Effectene (QIAGEN), and $10^6$ S2R+ cells in 1.6 mL of growth media. Knockdown was assessed by Western blotting at multiple time points. Strong knockdown of dynamin was observed after 8 d. To assess the effect of *shi* on Wg signaling, 1 mL of media containing or lacking Wg protein (see next section) was added 7 d after transfection. 1 d later, the cells were lysed to reconfirm protein knockdown and to assess luciferase levels using the Dual-Luciferase Reporter Assay System (Promega). For Rab5, however, only limited knockdown was observed using this protocol even after 8 d. To test the effect of Rab5, an alternative protocol was used. (2) 2.5 μg Super8XTOPFlash or Super8XFOPFlash and 25 ng pRL-CMV in 1.275 mL were sequentially combined with 20 μL Effectene Enhancer, 12.5 μL Effectene, 2.5 μg dsRNA, and $2 \times 10^6$ S2R+ cells in 2.5 mL of growth media. Knockdown was assessed by Western blotting at multiple time points. Strong knockdown of Rab5 was observed after 8 d. To assess the effect of Rab5 on Wg signaling, Wg-conditioned media was added, and cells were lysed as described in protocol 1. To induce Wg signaling using Wg DNA rather than Wg-conditioned media, the following protocols were used: (3) 1.25 μg Super8XTOPFlash or Super8XFOPFlash, 1.25 μg pMK33-Wg (a gift from N. Perrimon, Harvard Medical School, Boston, MA) or empty vector, and 12.5 ng pRL-CMV in 1.275 mL were sequentially combined with 20 μL Effectene Enhancer, 12.5 μL Effectene, 2.5 μg dsRNA, and $2 \times 10^6$ S2R+ cells in 2.5 mL of growth media. 4 or 8 d later, the cells were lysed to assess protein knockdown by Western blotting and luciferase levels. To test the effect of polIII-RL (DasGupta et al., 2005) and s-188-cc-RL (Hu et al., 2003), the following protocol was used: (4) 0.625 μg Super8XTOPFlash or Super8XFOPFlash, 1.25 μg pMK33-Wg or empty vector, and 0.625 μg polIII-RL or s-188-cc-RL in 1.275 mL were sequentially combined with 20 μL Effectene Enhancer, 12.5 μL Effectene, 2.5 μg dsRNA, and $2 \times 10^6$ S2R+ cells in 2.5 mL of growth media. 8 d later, the cells were lysed to assess protein knockdown by Western blotting and luciferase levels. To test the effect of tk-RL (Promega), the following protocol was used: (5) 1.13 μg Super8XTOPFlash or Super8XFOPFlash, 1.25 μg pMK33-Wg or empty vector, and 0.13 μg tk-RL in 1.275 mL were sequentially combined with 20 μL Effectene Enhancer, 12.5 μL Effectene, 2.5 μg dsRNA, and $2 \times 10^6$ S2R+ cells in 2.5 mL of growth media. 8 d later, the cells were lysed to assess protein knockdown by Western blotting and luciferase levels. All luciferase results are presented as the mean Super8XTOPflash/RL or Super8XFOPFlash/RL and SEM of multiple independent trials relative to the EGFP control (Table S2). Significance was based on a two-tailed *t* test.

### Wg media

To obtain media containing and lacking Wg protein, S2 Tub-Wg cells (Drosophila Genomics Resource Center) and S2 cells were grown in M3 Media (Sigma-Aldrich) with 1 g/L of yeast extract, 2.5 g/L bactopeptone, and 10% heat-inactivated FBS. 125 μg/ml hygromycin (Sigma-Aldrich) was added to the S2 Tub-Wg media. Cells were pelleted by centrifugation. Media was used immediately or stored at −80°C. The presence of Wg protein was confirmed by Western blotting.

### Western blot

Cells were washed with PBS and lysed in 1× Passive Lysis Buffer (Dual-Luciferase Assay; Promega) or radioimmunoprecipitation assay lysis buffer (0.150 M NaCl, 1% NP-40, 0.5% sodium deoxycholate, 0.1% SDS, and 0.05 M Tris, pH 8) supplemented with protease inhibitor cocktail (Complete). Proteins were quantified by Bradford assay. Blots were probed as described previously (Schulze et al., 1995) using the following antibodies: mouse antidynamin (1:2,000; BD Biosciences), mouse anti-actin (1:5,000; MP Biomedicals), mouse anti-Arm (1:2,500; Riggleman et al., 1990), mouse anti-Wg 4D4 (1:2,000; Brook and Cohen, 1996), and rabbit anti-Rab5 (1:500; Entchev et al., 2000). Secondary goat HRP-conjugated anti–mouse and anti–rabbit antibodies were used at 1:2,500 (Jackson ImmunoResearch Laboratories), and bands were visualized by Western lightning chemiluminescence plus reagent (PerkinElmer). Blots were developed in a processor (M35A X-OMAT; Kodak), scanned with a scanner (ScanMaker 8700; Microtek) and the accompanying ScanWizard Pro software (Microtek), and processed for brightness using Photoshop software (Adobe).

### *Drosophila* strains

Crosses were maintained at 21°C unless otherwise stated. Wing discs were equal in size to controls and morphologically normal unless otherwise stated. Representative wings of eclosed flies are shown. Wings were either mounted in Permount (Fisher Scientific) or just placed on a slide and visualized with a stereomicroscope (MZ16; Leica) fitted with a planApo 1× objective and a camera (Microfire; Optronics). Wing pictures were captured using Image-Pro Plus (MediaCybernetics) and In-Focus (Meyer). For curled wings, images were processed by extended focus in Image-Pro Plus. Images were recolored, adjusted for brightness, and painted to remove excess wings in Photoshop (Adobe). Expression patterns of *C96-Gal4* (Gustafson and Boulianne, 1996) and *C5-Gal4* (Yeh et al., 1995) were determined by crossing to *w; UAS-lacZ* and staining resultant larvae for β-galactosidase. Patterns did not alter with the cooverexpression of *UAS-wgHRP/TM6* (Dubois et al., 2001). To inhibit dynamin function, the Gal4 drivers were crossed to *w; TM3 UAS-shi$^{DN}$/TM6B Tb$^1$* (Moline et al., 1999). Our analysis of *shi$^{DN}$* expressed by *C5-Gal4* was performed on discs with relatively normal morphology, as changes in gross morphology were observed in some discs. *shi$^{ts1}$* mutant clones were generated by crossing *FRT18A shi$^{ts1}$* females to *w Ubi-GFPnls FRT18A; hsFLP* males and heat shocking the progeny for 1 h at 38°C 12–36 h after egg laying. Larvae were raised at 18°C and shifted to 35°C for 7 h immediately before dissection. Female larvae were processed as in conventional antibody staining (see next section) except that dissection and fixation were performed at the restrictive temperature to maintain a blockade in endocytosis. To affect early endosomal fusion, the Gal4 drivers were crossed to *UAS-Rab5$^{SN}$/SM5-TM6* (Entchev et al., 2000), *UAS-Rab5$^{QL}$/SM5-TM6* (a gift from M. Gonzalez-Gaitan, Max Planck Institute of Molecular Cell Biology and Genetics, Dresden, Germany), and *UAS-Rab5* (Entchev et al., 2000). Our analyses of *Rab5$^{SN}$* and *Rab5$^{QL}$* were performed on wing discs with relatively normal morphology, as changes in gross morphology were observed in many discs. *yw UAS-Arm$^{S10}$/+; UAS-Rab5$^{SN}$/+; C5-Gal4/+* (Pai et al., 1997) flies were dissected from pupal cases to examine wing morphology. Wild-type Rab5 overexpression was also analyzed by crossing *UAS-Rab5* to *yw hsFLP; Actin<y+<Gal4 UAS-GFP/SM5-TM6* and heat shocking progeny for 5–15 min at 38°C during early larval development. To generate *hrs* mitotic clones, *yw hsFLP; arm-LacZ FRT 40A* or *yw hsFLP; Ubi-GFP FRT 40A/CyO* males were crossed to *yw hsFLP; hrs$^{D28}$ FRT 40A/Gla Bc* females. Progeny were heat shocked at 38°C for 1 h during early first instar development. Because maternally deposited Hrs is very stable, the phenotypes described in this study may not be evident in small clones induced late in development. The overexpression of Hrs was studied using *C96-Gal4 UAS-hrs/TM6*, *C5-Gal4 UAS-hrs/TM6*, and *w; Sp/Cyo;*

*UAS-LampHRP* (a gift from H. Krämer, University of Texas Southwestern Medical Center at Dallas, Dallas, TX). Genetic interactions were examined using *yw; UAS-wg* (Wilder and Perrimon, 1995), *UAS-fz* (a gift from K. Bhat, Emory University School of Medicine, Atlanta, GA), and *w; Sp/CyO; UAS-dshMYC* (Penton et al., 2002). Wg signaling components were localized using the following stocks: *UAS-Myc-2xFYVE-GFP/CyO* (Wucherpfennig et al., 2003), *UAS-Rab7GFP/TM3* (Entchev et al., 2000), *UAS-wgHRP/TM6* (Dubois et al., 2001), *Tub-Gal4/TM6, hrs; Tub-Gal4/SM5-TM6*, and *UAS-ArrHA/TM6* (Culi and Mann, 2003).

**Immunohistochemistry and in situ hybridization**

For conventional antibody staining, wandering third instar larvae were dissected in PBS, fixed in 4% formaldehyde in PBS, and incubated in primary antibody overnight. The following primary antibodies were used: mouse anti-Wg 4D4 (1:10; Brook and Cohen, 1996), rabbit anti–β-galactosidase (1:1,000; Cappel), guinea pig anti-Sens (1:1,000; Nolo et al., 2000), mouse anti-Dll (1:500; a gift from G. Boekhoff-Falk, University of Wisconsin, Madison, WI), rabbit anti-Dll (1:100; Panganiban et al., 1994), mouse anti-HA (1:100; Covance), guinea pig anti-Spinster/Benchwarmer (1:100; Sweeney and Davis, 2002), and rat anti-Dsh CB (1:1,000; Shimada et al., 2001). Samples were later incubated in fluorescent conjugated secondary antibodies (1:300; Invitrogen and Jackson Immunochemicals). Samples were mounted in Vectashield mounting medium (Vector Laboratories) and were imaged using a confocal microscope (LSM 510; Carl Zeiss MicroImaging, Inc.) and accompanying software. Additional details of image acquisition and processing are shown in Table S3 (available at http://www.jcb.org/cgi/content/full/jcb.200510123/DC1). Control and experimental samples of each figure were taken at identical confocal settings. Single confocal sections of representative samples are shown unless otherwise stated. Extracellular protein staining was performed as described previously (Strigini and Cohen, 2000) using tubulin as a negative control. TUNEL labeling was performed as described previously (Wang et al., 1999) except that larvae were dissected in PBS and fixed in 4% formaldehyde in PBS. The TMR red In Situ Cell Death Detection Kit (Roche) was used. Changes in the columnar cell layer were evaluated. As a positive control, $y^1$ *w;* $Pr^1$ $Dr^1$*/TM3 Hs-Hid* $Sb^1$ larvae underwent a 1-h heat shock at 38°C 1 d before TUNEL staining (Fig. S1 H). In situ hybridization was performed as described previously (Verstreken et al., 2002) and mounted in 50% glycerol in PBS. Images were acquired with an imaging system (Imager.Z1; Carl Zeiss MicroImaging, Inc.) fitted with a 63× NA 1.4 plan-Apochromat lens and a camera (Axiocam MRm; Carl Zeiss MicroImaging, Inc.) using Axiovision software (Carl Zeiss MicroImaging, Inc.). Images were recolored using Photoshop (Adobe).

**Quantification**

To determine the extent of wing notching, the intact wing perimeter of each wing was measured using ImageJ software (National Institutes of Health) and divided by the respective total estimated wing perimeter. For each genotype, the mean and SEM were calculated. Significance was based on a two-tailed *t* test. To quantify the extent of protein colocalization in wing imaginal disc stainings, the number of colocalized pixels in a fixed area near the center of the wing pouch was measured using LabelVoxel and TissueStatistics functions of Amira (Indeed-Visual Concepts GmbH). Relative results are presented.

**Transmission electron microscopy**

*C5-Gal4/UAS-wgHRP* and *C5-Gal4* larvae were dissected in PBS and incubated in 0.5 g/L 3,3′-DAB (Sigma-Aldrich) + 0.003% $H_2O_2$ to visualize HRP. Samples were fixed in 2% PFA, 75 mM lysine, 10 mM NaIO, 37 mM phosphate buffer, pH 7.4, and postfixed in 3% $OsO_4$. Samples were dehydrated and embedded. 55-nm thin sections were stained in 4% uranyl acetate and then in 2.2% lead nitrate and 3.5% sodium citrate. Images were acquired with an electron microscope (JEM-1010; JEOL) fitted with a digital camera (2k; Gatan). No HRP-positive structures were detected apically in the C5-Gal4–negative control, indicating that the staining is specific for expressed Wg HRP. The *C5-Gal4/UAS-wgHRP* adult wing phenotype is consistent with increased Wg signaling, indicating that the fusion protein is functional.

**Online supplemental material**

Fig. S1 shows our analysis of cell death in wing discs with altered endocytosis by TUNEL. Fig. S2 shows the effect of the enhancement of Rab5-mediated endosomal fusion on Wg signaling. Table S1 describes the specific sequences of dsRNA used for knockdown in our cell culture assays. Table S2 provides quantitative data from the cell culture Wg signaling assay, including negative controls. Table S3 describes additional methods for image acquisition and processing. Online supplemental material is available at http://www.jcb.org/cgi/content/full/jcb.200510123/DC1.

We thank Y. Zhou for electron microscopy; S. DiNardo, P. Verstreken, and J. Vincent for discussions; and the Bloomington Stock Center, the University of Iowa Hybridoma Bank, P. Beachy, K. Bhat, G. Boekhoff-Falk, S. Cohen, M. Gonzalez-Gaitan, R. Nusse, N. Perrimon, and T. Uemura for reagents.

H.J. Bellen is supported by the Howard Hughes Medical Institute. This work was supported by a National Institute of General Medical Sciences grant (5R01 GM068949). E.S. Seto is supported by a National Institute of Environmental Health Sciences individual National Research Service Award (5F 30 ES11725) and is in the Baylor College of M.D./Ph.D. program.

Submitted: 24 October 2005
Accepted: 8 March 2006

## References

Altschuler, Y., S.M. Barbas, L.J. Terlecky, K. Tang, S. Hardy, K.E. Mostov, and S.L. Schmid. 1998. Redundant and distinct functions for dynamin-1 and dynamin-2 isoforms. *J. Cell Biol.* 143:1871–1881.

Baker, N.E. 1988. Transcription of the segment-polarity gene wingless in the imaginal discs of *Drosophila*, and the phenotype of a pupal-lethal wg mutation. *Development*. 102:489–497.

Bejsovec, A., and E. Wieschaus. 1995. Signaling activities of the *Drosophila* wingless gene are separately mutable and appear to be transduced at the cell surface. *Genetics*. 139:309–320.

Blair, S.S. 2005. Cell signaling: wingless and glypicans together again. *Curr. Biol.* 15:R92–R94.

Brennan, K., T. Klein, E. Wilder, and A.M. Arias. 1999. Wingless modulates the effects of dominant negative notch molecules in the developing wing of *Drosophila*. *Dev. Biol.* 216:210–229.

Brook, W.J., and S.M. Cohen. 1996. Antagonistic interactions between wingless and decapentaplegic responsible for dorsal-ventral pattern in the *Drosophila* Leg. *Science*. 273:1373–1377.

Bucci, C., R.G. Parton, I.H. Mather, H. Stunnenberg, K. Simons, B. Hoflack, and M. Zerial. 1992. The small GTPase rab5 functions as a regulatory factor in the early endocytic pathway. *Cell*. 70:715–728.

Bucci, C., P. Thomsen, P. Nicoziani, J. McCarthy, and B. van Deurs. 2000. Rab7: a key to lysosome biogenesis. *Mol. Biol. Cell*. 11:467–480.

Cadigan, K.M., and R. Nusse. 1997. Wnt signaling: a common theme in animal development. *Genes Dev.* 11:3286–3305.

Cliffe, A., F. Hamada, and M. Bienz. 2003. A role of Dishevelled in relocating Axin to the plasma membrane during Wingless signaling. *Curr. Biol.* 13:960–966.

Couso, J.P., M. Bate, and A. Martinez-Arias. 1993. A wingless-dependent polar coordinate system in *Drosophila* imaginal discs. *Science*. 259:484–489.

Couso, J.P., S.A. Bishop, and A. Martinez Arias. 1994. The wingless signalling pathway and the patterning of the wing margin in *Drosophila*. *Development*. 120:621–636.

Culi, J., and R.S. Mann. 2003. Boca, an endoplasmic reticulum protein required for wingless signaling and trafficking of LDL receptor family members in *Drosophila*. *Cell*. 112:343–354.

DasGupta, R., A. Kaykas, R.T. Moon, and N. Perrimon. 2005. Functional genomic analysis of the Wnt-wingless signaling pathway. *Science*. 308:826–833.

Dermaut, B., K.K. Norga, A. Kania, P. Verstreken, H. Pan, Y. Zhou, P. Callaerts, and H.J. Bellen. 2005. Aberrant lysosomal carbohydrate storage accompanies endocytic defects and neurodegeneration in *Drosophila* benchwarmer. *J. Cell Biol.* 170:127–139.

Diaz-Benjumea, F.J., and S.M. Cohen. 1995. Serrate signals through Notch to establish a Wingless-dependent organizer at the dorsal/ventral compartment boundary of the *Drosophila* wing. *Development*. 121:4215–4225.

Di Fiore, P.P., and P. De Camilli. 2001. Endocytosis and signaling: an inseparable partnership. *Cell*. 106:1–4.

Dubois, L., M. Lecourtois, C. Alexandre, E. Hirst, and J.P. Vincent. 2001. Regulated endocytic routing modulates wingless signaling in *Drosophila* embryos. *Cell*. 105:613–624.

Entchev, E.V., A. Schwabedissen, and M. Gonzalez-Gaitan. 2000. Gradient formation of the TGF-beta homolog Dpp. *Cell*. 103:981–991.

Fagotto, F., E. Jho, L. Zeng, T. Kurth, T. Joos, C. Kaufmann, and F. Costantini. 1999. Domains of axin involved in protein-protein interactions, Wnt pathway inhibition, and intracellular localization. *J. Cell Biol.* 145:741–756.

Gorfinkiel, N., G. Morata, and I. Guerrero. 1997. The homeobox gene Distalless induces ventral appendage development in *Drosophila*. *Genes Dev.* 11:2259–2271.

Gorvel, J.P., P. Chavrier, M. Zerial, and L. Gruenberg. 1991. rab5 controls early endosome fusion in vitro. *Cell*. 64:915–925.

Greco, V., M. Hannus, and S. Eaton. 2001. Argosomes: a potential vehicle for the spread of morphogens through epithelia. *Cell*. 106:633–645.

Gustafson, K., and G.L. Boulianne. 1996. Distinct expression patterns detected within individual tissues by the GAL4 enhancer trap technique. *Genome*. 39:174–182.

Hamada, F., Y. Tomoyasu, Y. Takatsu, M. Nakamura, S. Nagai, A. Suzuki, F. Fujita, H. Shibuya, K. Toyoshima, N. Ueno, and T. Akiyama. 1999. Negative regulation of Wingless signaling by D-axin, a *Drosophila* homolog of axin. *Science*. 283:1739–1742.

Hinshaw, J.E. 2000. Dynamin and its role in membrane fission. *Annu. Rev. Cell Dev. Biol.* 16:483–519.

Hu, X., L. Cherbas, and P. Cherbas. 2003. Transcription activation by the ecdysone receptor (EcR/USP): identification of activation functions. *Mol. Endocrinol.* 17:716–731.

Kasai, K., H.W. Shin, C. Shinotsuka, K. Murakami, and K. Nakayama. 1999. Dynamin II is involved in endocytosis but not in the formation of transport vesicles from the trans-Golgi network. *J. Biochem. (Tokyo)*. 125:780–789.

Klingensmith, J., R. Nusse, and N. Perrimon. 1994. The *Drosophila* segment polarity gene dishevelled encodes a novel protein required for response to the wingless signal. *Genes Dev.* 8:118–130.

Lin, H.V., D.B. Doroquez, S. Cho, F. Chen, I. Rebay, and K.M. Cadigan. 2003. Splits ends is a tissue/promoter specific regulator of Wingless signaling. *Development*. 130:3125–3135.

Lloyd, T., R. Atkinson, M.N. Wu, G. Pennetta, and H.J. Bellen. 2002. HRS is required for endosome to lysosome trafficking, and tyrosine kinase signaling. *Cell*. 108:261–269.

Lum, L., S. Yao, B. Mozer, A. Rovescalli, D. Von Kessler, M. Nirenberg, and P.A. Beachy. 2003. Identification of Hedgehog pathway components by RNAi in *Drosophila* cultured cells. *Science*. 299:2039–2045.

Marois, E., A. Mahmoud, and S. Eaton. 2006. The endocytic pathway and formation of the Wingless morphogen gradient. *Development*. 133:307–317.

Miaczynska, M., L. Pelkmans, and M. Zerial. 2004. Not just a sink: endosomes in control of signal transduction. *Curr. Opin. Cell Biol.* 16:400–406.

Moline, M.M., C. Southern, and A. Bejsovec. 1999. Directionality of wingless protein transport influences epidermal patterning in the *Drosophila* embryo. *Development*. 126:4375–4384.

Neumann, C.J., and S.M. Cohen. 1997. Long-range action of Wingless organizes the dorsal-ventral axis of the *Drosophila* wing. *Development*. 124:871–880.

Nolo, R., L.A. Abbott, and H.J. Bellen. 2000. Senseless, a Zn finger transcription factor, is necessary and sufficient for sensory organ development in *Drosophila*. *Cell*. 102:349–362.

Pai, L.M., S. Orsulic, A. Bejsovec, and M. Peifer. 1997. Negative regulation of Armadillo, a Wingless effector in *Drosophila*. *Development*. 124:2255–2266.

Panganiban, G., L. Nagy, and S.B. Carroll. 1994. The role of the Distal-less gene in the development and evolution of insect limbs. *Curr. Biol.* 4:671–675.

Parker, D.S., J. Jemison, and K.M. Cadigan. 2002. Pygopus, a nuclear PHD-finger protein required for Wingless signaling in *Drosophila*. *Development*. 129:2565–2576.

Peifer, M., D. Sweeton, M. Casey, and E. Wieschaus. 1994. wingless signal and Zeste-white 3 kinase trigger opposing changes in the intracellular distribution of Armadillo. *Development*. 120:369–380.

Penton, A., A. Wodarz, and R. Nusse. 2002. A mutational analysis of dishevelled in *Drosophila* defines novel domains in the dishevelled protein as well as novel suppressing alleles of axin. *Genetics*. 161:747–762.

Pfeiffer, S., S. Ricardo, J.B. Manneville, C. Alexandre, and J.P. Vincent. 2002. Producing cells retain and recycle Wingless in *Drosophila* embryos. *Curr. Biol.* 12:957–962.

Phillips, R.G., and J.R. Whittle. 1993. wingless expression mediates determination of peripheral nervous system elements in late stages of *Drosophila* wing disc development. *Development*. 118:427–438.

Piddini, E., F. Marshall, L. Dubois, E. Hirst, and J.P. Vincent. 2005. Arrow (LRP6) and Frizzled2 cooperate to degrade Wingless in *Drosophila* imaginal discs. *Development*. 132:5479–5489.

Raiborg, C., K.G. Bache, D.J. Gillooly, I.H. Madshus, E. Stang, and H. Stenmark. 2002. Hrs sorts ubiquitinated proteins into clathrin-coated microdomains of early endosomes. *Nat. Cell Biol.* 4:394–398.

Riggleman, B., P. Schedl, and E. Wieschaus. 1990. Spatial expression of the *Drosophila* segment polarity gene armadillo is posttranscriptionally regulated by wingless. *Cell*. 63:549–560.

Rulifson, E.J., and S.S. Blair. 1995. Notch regulates wingless expression and is not required for reception of the paracrine wingless signal during wing margin neurogenesis in *Drosophila*. *Development*. 121:2813–2824.

Schulze, K.L., K. Broadie, M.S. Perin, and H.J. Bellen. 1995. Genetic and electrophysiological studies of *Drosophila* syntaxin-1A demonstrate its role in nonneuronal secretion and neurotransmission. *Cell*. 80:311–320.

Seto, E.S., and H.J. Bellen. 2004. The ins and outs of Wingless signaling. *Trends Cell Biol.* 14:45–53.

Seto, E.S., H.J. Bellen, and T.E. Lloyd. 2002. When cell biology meets development: endocytic regulation of signaling pathways. *Genes Dev.* 16:1314–1336.

Seugnet, L., P. Simpson, and M. Haenlin. 1997. Requirement for dynamin during Notch signaling in *Drosophila* neurogenesis. *Dev. Biol.* 192:585–598.

Sharma, R.P., and V.L. Chopra. 1976. Effect of the Wingless (wg1) mutation on wing and haltere development in *Drosophila* melanogaster. *Dev. Biol.* 48:461–465.

Shimada, Y., T. Usui, S. Yanagawa, M. Takeichi, and T. Uemura. 2001. Asymmetric colocalization of Flamingo, a seven-pass transmembrane cadherin, and Dishevelled in planar cell polarization. *Curr. Biol.* 11:859–863.

Somsel Rodman, J., and A. Wandinger-Ness. 2000. Rab GTPases coordinate endocytosis. *J. Cell Sci.* 113:183–192.

Stenmark, H., R.G. Parton, O. Steele-Mortimer, A. Lutcke, J. Gruenberg, and M. Zerial. 1994. Inhibition of rab5 GTPase activity stimulates membrane fusion in endocytosis. *EMBO J.* 13:1287–1296.

Strigini, M., and S.M. Cohen. 2000. Wingless gradient formation in the *Drosophila* wing. *Curr. Biol.* 10:293–300.

Sweeney, S.T., and G.W. Davis. 2002. Unrestricted synaptic growth in spinster-a late endosomal protein implicated in TGF-beta-mediated synaptic growth regulation. *Neuron*. 36:403–416.

Tamai, K., M. Semenov, Y. Kato, R. Spokony, C. Liu, Y. Katsuyama, F. Hess, J.P. Saint-Jeannet, and X. He. 2000. LDL-receptor-related proteins in Wnt signal transduction. *Nature*. 407:530–535.

Teis, D., W. Wunderlich, and L.A. Huber. 2002. Localization of the MP1-MAPK scaffold complex to endosomes is mediated by p14 and required for signal transduction. *Dev. Cell*. 3:803–814.

Theisen, H., J. Purcell, M. Bennett, D. Kansagara, A. Syed, and J.L. Marsh. 1994. dishevelled is required during wingless signaling to establish both cell polarity and cell identity. *Development*. 120:347–360.

van den Heuvel, M., J. Klingensmith, N. Perrimon, and R. Nusse. 1993. Cell patterning in the *Drosophila* segment: engrailed and wingless antigen distributions in segment polarity mutant embryos. *Dev. Suppl.* 105–114.

van der Bliek, A.M., T.E. Redelmeier, H. Damke, E.J. Tisdale, E.M. Meyerowitz, and S.L. Schmid. 1993. Mutations in human dynamin block an intermediate stage in coated vesicle formation. *J. Cell Biol.* 122:553–563.

Veeman, M.T., D.C. Slusarski, A. Kaykas, S.H. Louie, and R.T. Moon. 2003. Zebrafish prickle, a modulator of noncanonical Wnt/Fz signaling, regulates gastrulation movements. *Curr. Biol.* 13:680–685.

Verstreken, P., O. Kjaerulff, T.E. Lloyd, R. Atkinson, Y. Zhou, I.A. Meinertzhagen, and H.J. Bellen. 2002. Endophilin mutations block clathrin-mediated endocytosis but not neurotransmitter release. *Cell*. 109:101–112.

Wang, S.L., C.J. Hawkins, S.J. Yoo, H.A. Muller, and B.A. Hay. 1999. The *Drosophila* caspase inhibitor DIAP1 is essential for cell survival and is negatively regulated by HID. *Cell*. 98:453–463.

Wehrli, M., S.T. Dougan, K. Caldwell, L. O'Keefe, S. Schwartz, D. Vaizel-Ohayon, E. Schejter, A. Tomlinson, and S. DiNardo. 2000. arrow encodes an LDL-receptor-related protein essential for Wingless signalling. *Nature*. 407:527–530.

Wilder, E.L., and N. Perrimon. 1995. Dual functions of wingless in the *Drosophila* leg imaginal disc. *Development*. 121:477–488.

Williams, J.A., S.W. Paddock, and S.B. Carroll. 1993. Pattern formation in a secondary field: a hierarchy of regulatory genes subdivides the developing *Drosophila* wing disc into discrete subregions. *Development*. 117:571–584.

Wodarz, A., and R. Nusse. 1998. Mechanisms of Wnt signaling in development. *Annu. Rev. Cell Dev. Biol.* 14:59–88.

Wucherpfennig, T., M. Wilsch-Brauninger, and M. Gonzalez-Gaitan. 2003. Role of *Drosophila* Rab5 during endosomal trafficking at the synapse and evoked neurotransmitter release. *J. Cell Biol.* 161:609–624.

Yanagawa, S., J.S. Lee, and A. Ishimoto. 1998. Identification and characterization of a novel line of *Drosophila* Schneider S2 cells that respond to wingless signaling. *J. Biol. Chem.* 273:32353–32359.

Yeh, E., K. Gustafson, and G.L. Boulianne. 1995. Green fluorescent protein as a vital marker and reporter of gene expression in *Drosophila*. *Proc. Natl. Acad. Sci. USA*. 92:7036–7040.

Zecca, M., K. Basler, and G. Struhl. 1996. Direct and long-range action of a wingless morphogen gradient. *Cell*. 87:833–844.